

Determination of the tunneling electron-phonon spectral function in high- T_c superconductors with energy dependence of the normal density of states.

R.S. Gonnelli,¹ G.A. Ummarino,¹ and V.A. Stepanov²

¹*INFN—Dipartimento di Fisica, Politecnico di Torino, 10129 Torino, Italy*

²*P.N. Lebedev Physical Institute, Russian Academy of Sciences, Moscow, Russia*

Abstract

In the present paper we discuss the limits and the correct utilization of the standard program for the inversion of Eliashberg equations and the determination of the electron-phonon spectral function and the coulomb pseudopotential from tunneling measurements in high- T_c superconductors. In order to compare the calculated density of states with the experimental one, we introduce the results of the inversion procedure, applied to our recent tunneling data in $\text{Bi}_2\text{Sr}_2\text{CaCu}_2\text{O}_{8+x}$ single-crystal break junctions with $T_c = 93$ K, in a direct program for the solution of Eliashberg equations. Most of the observed differences between theoretical and experimental curves at energy greater than gap can be explained by a smooth energy dependence of the normal density of states that we introduced in the direct solution of the Eliashberg equations. Finally we show that the effects of the energy-dependent normal density of states can be simulated by an efficient electron-phonon spectral function but, also, by a negative, nonphysical, coulomb pseudopotential.

PACS numbers: 74.50.+r; 74.70.Vy

Keywords: Eliashberg equations, electron-phonon coupling, phonon mechanism

Typeset using REVTeX

I. INTRODUCTION

At the present time it can be regarded as a well-established fact that in the oxide superconductors, as in conventional ones, and at temperatures below the critical temperature T_c , the charge carriers are bound in pairs in an energy band whose width is of the order of the gap, but the mechanism responsible for the attraction between the charges has still not been identified.

A very important method for obtaining information concerning this aspect is constituted by tunnel spectroscopy measurements [1–4], that, through the Eliashberg equations (EE) inversion, allow to determine the electron-phonon spectral function, $\alpha^2(\omega)F(\omega)$, of the material. Seven years after the publication of the first, tentative, $\alpha^2(\omega)F(\omega)$ curves obtained by inversion of the gap equations from point-contact tunneling data in $\text{Bi}_2\text{Sr}_2\text{CaCu}_2\text{O}_{8+x}$ (BSCCO) [5,6], a certain skepticism still persists on the possibility of obtaining a reliable and reproducible $\alpha^2(\omega)F(\omega)$ from tunneling data in BSCCO. The main reasons for this skepticism are related to: i) the determination of the low-temperature normal-state conductance that is a fundamental ingredient for the inversion of the gap equations, but it is not a measurable quantity in this high- T_c superconductor and ii) the considerable deviations of the dI/dV curves from the ideal BCS behaviour, observed in this material up to short time ago. More recently, tunneling experiments using the break-junction approach have shown that single crystals of very high structural and crystallographic quality and a very fine technique for the production of stable and reproducible junctions can lead to BCS-like lifetime-broadened results [3,4]. In this case the deviations of the BSCCO break-junction dI/dV characteristics from the ideal Superconductor-Insulator-Superconductor (SIS) behaviour are relatively small. After an unfolding procedure for extracting the density of states N_S from the SIS tunneling conductance, it is possible to observe that most of the deviations of N_S from the BCS density of states can be explained in all the energy range only by the presence of a certain amount of lifetime broadening [7]. Similar results have been recently obtained with the point-contact technique by using highly doped GaAs as counterelectrode [2].

In this work we develop a method for the correct utilization of the best experimental tunneling data in the inversion of the EE, by introducing different theoretical energy-dependent normal densities of states (NDOS) determined by suitable criteria we will discuss in detail in section III. In this way we have calculated $\alpha^2(\omega)F(\omega)$, the coulomb pseudopotential μ^* and other observable physical quantities that depend on the first two, for every normal density of states. Then we have put $\alpha^2(\omega)F(\omega)$ and μ^* in a direct program for the solution of the EE and, for each different NDOS, we calculated the superconductive quasiparticle density of states (DOS) for comparison with the experimental data. Some possible explanations for the discrepancies between theoretical and experimental DOS are given. By using the direct program and including the effect of an energy-dependent symmetric NDOS of proper shape, we find that the agreement with the experimental data improves very much at energies greater than gap. Finally, from the theoretical DOS calculated by the direct program with an energy-dependent NDOS, and by using again the standard inversion program we determine the efficient values of $\alpha^2(\omega)F(\omega)$ and μ^* , that simulate the effects of the NDOS depending on energy. From now on we set $\hbar = c = k_B = 1$.

II. INVERSION OF THE ELIASHBERG EQUATIONS

The experimental data that we use in order to extract the $\alpha^2(\omega)F(\omega)$ and to compare with the theoretical DOS have been obtained by employing the break-junction technique on BSCCO single crystals of very high crystallographic and chemical quality, as indicated by x-ray diffractograms, resistivity versus temperature and susceptibility measurements. Before breaking the crystals, their $R(T)$ characteristics were measured and the critical temperature was $T_c = 93$ K with $\Delta T_c(10 - 90\%) = 2$ K. Immediately afterwards, at 4.2 K, a finely controlled bending force was applied to the thin sample holder which the crystal was mounted on. It produced the break of the very thin crystal (about $1 \times 1 \times 0.02$ mm³) perpendicularly to the ab planes and the creation of the junction. By varying the bending force it was possible to reproducibly and accurately control the resistance of the junction and also the

$I(V)$ curves were very stable and reproducible. All the details concerning the experimental data and the reproducible determination of the density of states and the Eliashberg function in these crystals can be found in a forthcoming paper [8]. Among several $I(V)$ tunneling measurements of very high quality we selected one of the best and applied an unfolding procedure for extracting the quasiparticle density of states N_S from the SIS tunneling conductance. Figure 1 shows that the quality of the experimental DOS (open circles) is largely improved with respect to the measurements of few years ago and, in particular, sharp peaks at the energy gap Δ and an almost constant N_S at $eV \gg \Delta$ are now present. Nevertheless, it is possible to observe that deviations of N_S from the "pure" BCS density of states N_{BCS} are still present: it is a problem for the inversion of EE [9–14] because very large oscillations in $N_{rid} = N_S/(N_n \cdot N_{BCS}) - 1$ (where N_n is the normal density of states) produce singularity and no convergence at the increase of the number of iterations when the standard inversion program is used [13,14]. Usually this difficulty in the calculation of the reduced density of states N_{rid} is overcome by using the lifetime-broadened expression [4–6,8] instead of N_{BCS} : $N_l(\omega) = \text{real} \left\{ (\omega - i\Gamma) / \sqrt{(\omega - i\Gamma)^2 - \Delta(0)^2} \right\}$. The values of the energy gap $\Delta(0)$ and of the lifetime broadening parameter Γ that fit the experimental density of states of Fig. 1 are $\Delta(0) = 23$ meV, $\Gamma = 2.9$ meV and, consequently, $2\Delta(0)/T_c = 5.74$. In Fig. 1 the solid line represents the lifetime broadening fit of the experimental data.

Even if widely used as a first approximation for the $\alpha^2(\omega)F(\omega)$ determination, the procedure of using $N_l(\omega)$ instead of N_{BCS} appears somehow incoherent. In fact, some parts of the inversion program contain the ideal reference curve, N_{BCS} , but, for calculating N_{rid} , a different curve N_l is used. For a fully coherent utilization of the inversion program it is necessary to compare the experimental data to the ideal BCS behaviour. We also believe that it is fundamental to normalize the experimental data to an energy-dependent NDOS and then calculate the N_{rid} by using the N_{BCS} as reference. In high- T_c superconductors (HTS) like BSCCO, the normal conductance is unknown at the temperature of measurement, for example $T_{ex} = 4.2$ K, since the upper critical magnetic field necessary to suppress the superconducting phase is very large and unrealizable, while, on the other hand, $\Delta T = T_c - T_{ex}$

is too large to consider $\text{NDOS}(T_c) \simeq \text{NDOS}(T_{ex})$. For this reason, we will use four simple arbitrary expressions for the NDOS with three free parameters each, to be determined by suitable physical conditions. Comparing the results of this approach to the experimental data of Fig. 1 we will select the NDOS that, possibly, will be the most plausible one for our break-junction tunneling experiment.

III. ENERGY DEPENDENCE OF THE NORMAL DENSITY OF STATES

The HTS have a very complicated crystallographic structure. Ho et al. [15] have given general motivations to the fact that six or more atoms of the transition elements for unitary cell may produce definite peaks in the NDOS. There are also many experimental results indicating this hypothesis as correct [8,16,17]. In particular the results of Mandrus et al. in BSCCO [18] and our recent measurements in $\text{Bi}_2\text{Sr}_2\text{CuO}_{6+x}$ single crystals suggest an energy dependence of the NDOS which varies with the direction of the tunneling process (ab plane or c axis). Since the exact dependence is unknown, we used four different, but symmetric, analytical forms for the energy dependence of the NDOS: exponential, linear, parabolic and lorentzian

$$N_n^{\text{exp}}(\omega) = \frac{N(0)}{1+x} \left[1 + x \cdot \exp\left(\frac{-|\omega|}{a}\right) \right] \quad (3.1)$$

$$N_n^{\text{lin}}(\omega) = \frac{N(0)}{1+x} \left[1 + x \cdot \theta(a - |\omega|) \cdot \left(1 - \frac{|\omega|}{a}\right) \right] \quad (3.2)$$

$$N_n^{\text{par}}(\omega) = \frac{N(0)}{1+x} \left[1 + x \cdot \theta(a - |\omega|) \cdot \left(1 - \frac{|\omega|^2}{a^2}\right) \right] \quad (3.3)$$

$$N_n^{\text{lor}}(\omega) = \frac{N(0)}{1+x} \left[1 + \frac{x \cdot a^2}{a^2 + \omega^2} \right] \quad (3.4)$$

where $N(0)$, a and x are free parameters. $N(0)$ is the density of states at the Fermi level and x controls the behaviour of the DOS at large energies. In the best tunneling measurements along the ab plane, it is reasonable to consider $x \geq 0$, i.e. the tunneling conductance is

constant or slightly decreasing at large energies, both for experimental reasons [3,4,8,18] and because the total isotope effect is less than 1/2 in HTS and this implies $\partial^2 N_n(\omega)/\partial\omega^2|_{\omega=0} < 0$ [19]. Of course in all the Eqs. 3.1-3.4, $N_n(\omega) = N(0)$ when ω tends to zero.

For determining the values of the parameters we employ the following conditions:

a) $\lim_{\omega \rightarrow +\infty} N_S(\omega) = \lim_{\omega \rightarrow +\infty} N_n(\omega) = N_{ex}(+\infty)$

where $N_{ex}(+\infty)$ is the experimental density of states at energy $\omega \gg \Delta(0)$;

b) $\int_0^{+\infty} N_{ex}(\omega) d\omega = \int_0^{+\infty} N_n(\omega) d\omega$

which expresses the law of conservation for the number of states;

c) $\int_{\Delta(0)}^{+\infty} \{N_{ex}(\omega)/[N_n(\omega) \cdot N_{BCS}(\omega)] - 1\} d\omega \simeq 0$

since the oscillations of the experimental "normalized" data around the ideal BCS curve in the phonon energy range should be symmetric [1,20].

The condition b is ideal: in reality the experimental curve shows a small zero-bias conductance and we have applied this modified condition:

b') $\int_0^{\omega_m} N_{ex}(\omega) d\omega - A_{lc} = \int_0^{\omega_m} N_n(\omega) d\omega$

where ω_m is the highest energy of the experimental data and $A_{lc} = c \cdot \omega_m$ with $0 \leq c \leq N_{ex}(0)$ is a small contribution eventually produced by leakage currents.

In the same way, for the practical estimation of the parameters, the condition c becomes:

c') $\min \left| \int_{\Delta_m}^{+\infty} \{N_{ex}(\omega)/[N_n(\omega) \cdot N_{BCS}(\omega)] - 1\} d\omega \right|$

where $\Delta_m > \Delta(0)$ is the first point of the experimental data used in the standard procedure for the inversion of the Eliashberg equations.

In the case of our experimental data shown in Fig. 1, a program for the numerical calculation of the parameters according to the conditions a, b' and c' yields :

	$N(0)(\Omega^{-1})$	x	$a(meV)$	$A_{lc}(meV \cdot \Omega^{-1})$
exp	$6.099 \cdot 10^{-2}$	0.108	52	0.403
lin	$6.635 \cdot 10^{-2}$	0.206	70	0.288
par	$6.230 \cdot 10^{-2}$	0.132	69	0.345
lor	$6.200 \cdot 10^{-2}$	0.127	35	0.368

The different, energy-dependent NDOS curves corresponding to the parameters of the table are shown in Fig. 2. If we know the $I(V)$ curve for $T \geq T_c$, in order to check the quality of the fit for $N_n(\omega)$, we can use the well-known expression of the tunnel current of a symmetric junction:

$$I(V) = e^{-1} G_{NN} \cdot \int_{-\infty}^{+\infty} N_n(\omega) N_n(\omega + eV) [f(\omega) - f(\omega + eV)] d\omega$$

where G_{NN} is a constant and $f(\omega)$ is the Fermi function. Since G_{NN} is unknown, we can use the quantity $I(V)/[\partial I(V)/\partial V]$ for a comparison of the theoretical results with the experimental data.

Now we can correctly calculate the $N_{rid} = N_{ex}(\omega)/[N_n(\omega) \cdot N_{BCS}(\omega)] - 1$ and, by the standard inversion program [13], we can determine the spectral function $\alpha^2(\omega)F(\omega)$, the coulomb pseudopotential μ^* , the electron-phonon interaction constant $\lambda = \int_0^{+\infty} [\alpha^2(\omega)F(\omega)/\omega] d\omega$, T_c , the area A of $\alpha^2(\omega)F(\omega)$, the coefficient b of the quadratic part of $\alpha^2(\omega)F(\omega)$ for $\omega \rightarrow 0$ and ω_c , that is the cut-off frequency. The results of this inversion procedure, applied to the experimental data of Fig. 1, are summarized in the following table for the different energy-dependent NDOS curves:

	λ	μ^*	$A(meV)$	$T_c(K)$	$b(meV^{-2})$	$\omega_c(meV)$
exp	3.34	$0.93 \cdot 10^{-2}$	47.21	93.6	$3.9 \cdot 10^{-3}$	225
lin	2.86	$0.26 \cdot 10^{-1}$	47.68	99.7	$1.6 \cdot 10^{-3}$	225
par	3.03	$0.31 \cdot 10^{-1}$	48.40	98.8	$2.7 \cdot 10^{-3}$	225
lor	3.24	$0.31 \cdot 10^{-1}$	47.49	94.6	$3.0 \cdot 10^{-3}$	225

In Fig. 3 the spectral functions $\alpha^2(\omega)F(\omega)$ for the different NDOS models are compared to the generalized phonon density of states $G(\omega)$ of BSCCO [21].

By solving the standard Eliashberg equations in direct way we can now check if the different $\alpha^2(\omega)F(\omega)$ and μ^* reproduce the experimental density of states $N_{ex}(\omega)$. The well-known standard EE are:

$$\Delta(\omega)Z(\omega) = \int_0^{\omega_c} P(\omega') \cdot [K_+(\omega, \omega') - \mu^*] d\omega' \quad (3.5)$$

$$[1 - Z(\omega)] \cdot \omega = \int_0^\infty N_S(\omega') \cdot K_-(\omega, \omega') d\omega' \quad (3.6)$$

where

$$K_\pm(\omega, \omega') = \int_0^{+\infty} \alpha^2(\Omega) F(\Omega) \cdot \left[\frac{1}{\omega' + \omega + \Omega + i \cdot \delta} \pm \frac{1}{\omega' - \omega + \Omega - i \cdot \delta} \right] d\Omega$$

and $P(\omega) = \text{Real} \left(\Delta(\omega) / \sqrt{\omega^2 - \Delta^2(\omega)} \right)$ is the pair density of states, while $N_S(\omega) = \text{Real} \left(\omega / \sqrt{\omega^2 - \Delta^2(\omega)} \right)$ is the quasiparticle one.

Figures 4 (a), 4 (b), 5 (a) and 5 (b) show a comparison of the densities of states calculated for $N_n(\omega) = \text{cost}$ by solving Eqs. 3.5 and 3.6 (dash-dot lines) with the normalized experimental ones (open circles) and with the densities of states calculated by the modified EE that take into account the four different models for $N_n(\omega)$ as it will be discussed in the following (solid lines). Discrepancies between the theoretical DOS for $N_n(\omega) = \text{cost}$ and the normalized experimental curve are remarkable for all the different forms of $N_n(\omega)$. They can be due to the inversion procedure as well as to the form of the Eliashberg equations.

For what concerns the inversion program, it is necessary to remember that:

- 1) The true normal conductance can be more cumbersome than the theoretical one and, as a consequence, N_{rid} may be not correct.
- 2) The standard inversion program was made for ideal BCS-like curves, not for gapless, broadened ones.
- 3) The dispersion relations, used in the standard program for calculating $\text{Real}(\Delta(\omega))$ and $\text{Im}(\Delta(\omega))$ [13,14], are incorrect if $N_{ex}(0) \neq 0$.
- 4) In the standard inversion program $\lim_{\omega \rightarrow 0} \alpha^2(\omega) F(\omega) = \lim_{\omega \rightarrow 0} b \cdot \omega^2$ (parabolic behaviour) whereas in superconductors with bidimensional character like BSCCO we can expect a linear behaviour: $\lim_{\omega \rightarrow 0} \alpha^2(\omega) F(\omega) = \lim_{\omega \rightarrow 0} a \cdot \omega$.
- 5) The energy dependence of the normal density of states is neglected in the standard inversion program, i.e. $N_n(\omega) = N(0)$.

Concerning the Eliashberg equations it should be born in mind that:

- 1) The Migdal's theorem is no more valid in HTS since the Debye phonon frequency is of the order of the Fermi energy [22].

2) The Eliashberg equations in the simple form expressed by Eqs. 3.5 and 3.6 are valid only for homogeneous and isotropic three-dimensional superconductors whereas BSCCO is bidimensional and very anisotropic.

3) The order parameter is supposed to be in s-wave symmetry.

4) The coulomb pseudopotential is considered constant but it could be energy dependent [23].

5) In the simple, standard form of the Eliashberg equations $N_n(\omega) = N(0)$.

In spite of the previous assertions, we assume two fundamental hypotheses:

a) The standard inversion program provides results approximately correct for what concerns $\alpha^2(\omega)F(\omega)$ and μ^* .

b) The differences between experimental and theoretical curves at $\omega > \Delta$ can be explained by putting $N_n(\omega) \neq N(0)$.

The new Eliashberg equations that take into account the energy dependence of the normal density of states at $T = 0$ are [24–28]:

$$\Delta(\omega)Z(\omega) = \int_0^{\omega_c} n_1(\omega') \cdot [K_+(\omega, \omega') - \mu^*] d\omega',$$

$$[1 - Z(\omega)] \cdot \omega = \int_0^{+\infty} n_2(\omega') \cdot K_-(\omega, \omega') d\omega',$$

$$\chi(\omega) = \int_0^{+\infty} n_3(\omega') \cdot K_+(\omega, \omega') d\omega'.$$

The normal density of states depending on energy $\rho(\omega) = N_n(\omega)/N(0)$ enters through three functions defined as:

$$n_1(\omega) = \left(-\frac{1}{\pi}\right) \text{Im} \left(\int_{-\infty}^{+\infty} \rho(\omega') \cdot \frac{\Delta(\omega) \cdot Z(\omega)}{D(\omega, \omega')} d\omega' \right),$$

$$n_2(\omega) = \left(-\frac{1}{\pi}\right) \text{Im} \left(\int_{-\infty}^{+\infty} \rho(\omega') \cdot \frac{\omega \cdot Z(\omega)}{D(\omega, \omega')} d\omega' \right),$$

$$n_3(\omega) = \left(\frac{1}{\pi}\right) \text{Im} \left(\int_{-\infty}^{+\infty} \rho(\omega') \cdot \frac{\omega' + \chi(\omega)}{D(\omega, \omega')} d\omega' \right)$$

where $D(\omega, \omega') = Z^2(\omega) \cdot [\omega^2 - \Delta^2(\omega)] - [\omega' + \chi(\omega)]^2$.

Energies are measured from the chemical potential and the real part of $\chi(\omega)$ represents a shift of the chemical potential due to the electron-phonon interaction. The energy-dependent electronic density of states $\rho(\omega)$ modulates the pair density of states $N(0) \cdot n_1(\omega)$ and the quasiparticle one $N(0) \cdot [n_2(\omega) - n_3(\omega)]$. In this article, only for simplicity, we have supposed that all the normal densities of states are symmetric: $N_n(\omega) = N_n(-\omega)$ and this produces $\chi(\omega) = 0$.

IV. RESULTS AND DISCUSSION

The theoretical $N_S(\omega)/N(0)$ curves for $N_n(\omega) \neq \text{const}$ (solid lines) are compared to the experimental normalized curves (open circles) in Figs. 4 (a, b) and 5 (a, b) for exponential, linear, parabolic and lorentzian cases, respectively. The same figures also show the normal densities of states $N_n(\omega)$ (dot lines) and $N_{BCS}(\omega)/(1+x)$ (dash lines) for the four above mentioned models. We can see that the agreement between the theoretical and the experimental normalized DOS is particularly good for the exponential and the linear cases (Figs. 4 (a) and 4 (b), respectively).

The gap value and the ratio $2\Delta(0)/T_c$ are modified by the energy dependence of the NDOS as it is shown in the following table:

	$\Delta(0)(meV)$	$2\Delta(0)/T_c$
exp	21.0	5.24
lin	20.0	4.99
par	21.2	5.27
lor	21.3	5.31

As it has been predicted in a previous work [28], a negative curvature of the energy-dependent NDOS produces a reduction of the gap $\Delta(0)$.

The best case seems to be the exponential one where $\lambda = 3.34$, $\mu^* = 0.93 \cdot 10^{-2}$, $T_c = 93.6$ K. We remind that the experimental value of T_c is 93 K. In our opinion,

these results are remarkable because μ^* is small but positive, T_c is coincident with the experimental one and λ is not too large: the amorphous low- T_c superconductor $\text{Pb}_{0.5}\text{Bi}_{0.5}$ has $\lambda = 3.00$ and $2\Delta(0)/T_c = 5.19$ [10]. Moreover if we calculate the electron-phonon coupling constant by using the following self-consistent formula [15,29] for $T = 0$ K: $\lambda = 2 \int_0^{+\infty} d\omega' N_n(\omega') \int_0^{+\infty} d\Omega \frac{\alpha^2(\Omega)F(\Omega)}{(\Omega-\omega')^2}$ we obtain $\lambda = 2.69$. It is correct to remember that T_c is calculated by the EE with $N_n(\omega) = N(0)$, but, since $N_n(\omega)$ has not a definite peak near the Fermi level, the value of T_c is not significantly affected by the energy dependence of the NDOS [28]. In Fig. 6 the experimental data (open circles) are compared to the theoretical electron density of states for the exponential case (solid line) in the full positive energy range. The agreement of the two curves for $\omega > 25$ meV is very good.

Similar results have been obtained in 6 additional break-junction tunneling curves measured on the same BSCCO single crystals with $T_c = 93$ K. The dI/dV curves suitable for the analysis previously described were selected among all the measured data by using some criteria that can be summarized as follows: i) Presence of sharp and symmetric gap structures; ii) Presence of symmetric and clear phonon-like structures; iii) Presence of a background conductance smoothly decreasing with energy at $\omega > 25$ meV. In all the cases the use of the exponential energy dependence of Eq. 3.1 for the normal density of states gave the best agreement between the theoretical DOS and the experimental one. The electron-phonon spectral functions $\alpha^2(\omega)F(\omega)$ obtained by the inversion of the Eliashberg equations in these 6 additional cases show large similarities to the $\alpha^2(\omega)F(\omega)$ of Fig. 3 (solid line) and the calculated average values of λ and T_c present a small variance of the order of $\pm 11\%$ and $\pm 2.7\%$, respectively [8].

An interesting question is whether it is possible to reproduce the tunneling characteristics for $N_n(\omega) \neq \text{const}$ within the framework of the usual Eliashberg theory. For trying to give an answer we considered the $N_{rid}(\omega)$ calculated by the direct program for $N_n(\omega) = N_n^{\text{exp}}(\omega)$ and, by using the standard inversion program, found an effective electron-phonon spectral function $\alpha^2(\omega)F(\omega)_{eff}$ and a μ_{eff}^* that simulate the energy dependence of the normal density of states. The results are shown in Fig. 7 where the effective electron-phonon spectral

function is represented as a dash line while the original $\alpha^2(\omega)F(\omega)$ determined from experimental data (after normalization with $N_n^{\text{exp}}(\omega)$) is shown as a solid line and the open circles represent the neutron generalized phonon density of states. We obtained $\lambda_{eff} = 3.4$, $\mu_{eff}^* = -0.31 \cdot 10^{-1}$, $T_{ceff} = 94$ K, $A_{eff} = 40.7$ meV, $b_{eff} = 9 \cdot 10^{-3} \text{meV}^{-2}$.

Finally, Figure 8 shows the electron-phonon coupling factor $\alpha^2(\omega)$ as determined from the data shown in Fig. 7. We can observe that $\alpha^2(\omega)$ determined from experimental data (solid line) has a large energy dependence which suggests the presence of a strong electron-phonon coupling with phonon modes between 12 and 27 meV and between 60 and 80 meV, while the coupling appears rather depressed for phonon modes between 29 and 56 meV. Similar results have been obtained in previous break-junction tunneling experiments in BSCCO and can be explained by the possible directionality mainly along the ab plane of the tunneling process in our break junctions [4,8]. Moreover, in Fig. 8 it can be seen that not to consider the energy dependence of the NDOS (i.e. to use the standard program for the inversion of the EE on the DOS obtained by the direct solution in presence of the NDOS energy dependence) produces an effective coupling factor $\alpha^2(\omega)_{eff}$ (dash line) that overestimates the soft phonon modes and gives rise to a little and negative nonphysical value of the coulomb pseudopotential.

In conclusion, we have seen that in order to obtain plausible values for $\alpha^2(\omega)F(\omega)$, λ , μ^* and T_c it is necessary to use the standard program for the inversion of EE in a correct and coherent way. The effect of a nonconstant NDOS on the normalized tunneling conductance is significant and cannot be accounted for in a meaningful way within the framework of the standard Eliashberg theory without obtaining effective parameters $\alpha^2(\omega)F(\omega)_{eff}$ and μ_{eff}^* that alter the physical interpretation of the problem. Finally, a strong electron-phonon interaction, restricted to some particular phonon modes of the $G(\omega)$, and a smooth energy dependence of the NDOS permit to explain our recent break-junction tunneling data in BSCCO at $\omega > \Delta$ in an excellent way. In the next future, it will be necessary to include in the EE the effect of anisotropy and of the bidimensional character of Bi-based high- T_c superconductors, as well as, to calculate the effect of the breakdown of Migdal's theorem on the critical temperature and on the superconducting gap by using the electron-phonon

spectral functions $\alpha^2(\omega)F(\omega)$ reproducibly determined in this and in previous experiments.

V. ACKNOWLEDGEMENTS

Many thanks are due to M. Pescarolo for the help in performing the break-junction tunneling measurements.

REFERENCES

- [1] E.L. Wolf, *Principles of electron tunneling spectroscopy* (Oxford University Press, New York, 1985).
- [2] D. Shimada, Y. Shiina, A. Mottate, Y. Ohjagi and N. Tsuda, Phys. Rev. B **51** (1995) 16495.
- [3] S.I. Vedeneev, A.A. Tsvetkov, A.G.M. Jansen and P. Wyder, Physica C **235-240** (1994) 1851.
- [4] R.S. Gonnelli, S.I. Vedeneev, O.V. Dolgov and G.A. Ummarino, Physica C **235-240** (1994) 1861.
- [5] S.I. Vedeneev and V.A. Stepanov, Physica C **162-164** (1989) 1131.
- [6] R.S. Gonnelli, L.N. Bulaevskii, O.V. Dolgov and S.I. Vedeneev, in *High Temperature Superconductivity*, eds. C. Ferdeghini and A.S. Siri (World Scientific, Singapore, 1990), 194.
- [7] R.C. Dynes, V. Narayanamurti and J.P. Garno, Phys. Rev. Lett. **41** (1978) 1509.
- [8] R.S. Gonnelli et al., to be published.
- [9] G.M. Eliashberg, Sov. Phys. JETP **3** (1963) 696.
- [10] J.P. Carbotte, Rev. Mod. Phys. **62** (1990) 1028.
- [11] P.B. Allen and B. Mitrovich, *Theory of superconducting T_c* , in Solid State Physics, Vol. **37** (Academic Press, New York, 1982).
- [12] R.D. Parks, *Superconductivity* (Marcel Dekker, New York, 1969).
- [13] V.M. Svistunov, A.I. D'yachenko and M.A. Belogolovskii, J. Low. Temp. Phys. **31** (1978) 339.
- [14] A.A. Galkin, A.I. D'yachenko and V.M. Svistunov, Sov. Phys. JETP **39** (1974) 1115.

- [15] K.M. Ho, M.L. Cohen and W.E. Pickett, Phys. Rev. Lett. **41** (1978) 815.
- [16] Qiang Huang, J.F. Zasadzinski, K.E. Gray, J.Z. Liu and H.Claus, Phys. Rev. B **40** (1989) 9366.
- [17] Takuya Matsumoto, Supab Choopun and Tomoji Kawai, Phys. Rev. B **52** (1995) 591.
- [18] D. Mandrus, L. Forro, D. Koller and L. Mihaly, Nature **351** (1991) 460.
- [19] R. Kishore, Phys. Lett. A **205** (1995) 244.
- [20] P. Ochik, V.M. Svistunov, M.A. Belogolovskii and A.I. D'yachenko, Sov. Phys. Solid. St. **20** (1978) 1101.
- [21] B. Renker, F. Gompf, D. Ewert, P. Adelmann, H. Schmidt, E. Gering and H. Mutka, Z. Phys. B **77** (1989) 65.
- [22] C. Grimaldi, L. Pietronero and S. Strässler, Phys. Rev. Lett. **75** (1995) 1158.
- [23] M. Dayan, Physica C **167** (1990) 228.
- [24] B. Mitrovich and J.P. Carbotte, Solid State Comm. **40** (1981) 249.
- [25] B. Mitrovich and J.P. Carbotte, Can. J. Phys. **61** (1983) 784.
- [26] W.E. Pickett, Phys. Rev. B **21** (1980) 3897.
- [27] Yasushi Yokoya, Physica C **231** (1994) 341.
- [28] Yasushi Yokoya and Yoshiko Oi Nakamura, Physica C **248** (1995) 83.
- [29] B. Mitrovich and J.P. Carbotte, Can. J. Phys. **61** (1983) 758.

FIGURES

FIG. 1. Quasiparticle density of states determined from the tunneling conductance of a single-crystal $\text{Bi}_2\text{Sr}_2\text{CaCu}_2\text{O}_{8+x}$ break junction.

FIG. 2. Comparison between the four different energy-dependent normal densities of states used in this paper and described in Eqs. 3.1 - 3.4.

FIG. 3. Spectral functions $\alpha^2(\omega)F(\omega)$ determined by using the standard program of inversion of the Eliashberg equations for the different NDOS models of Fig. 2 compared to the generalized phonon density of states $G(\omega)$ (open circles).

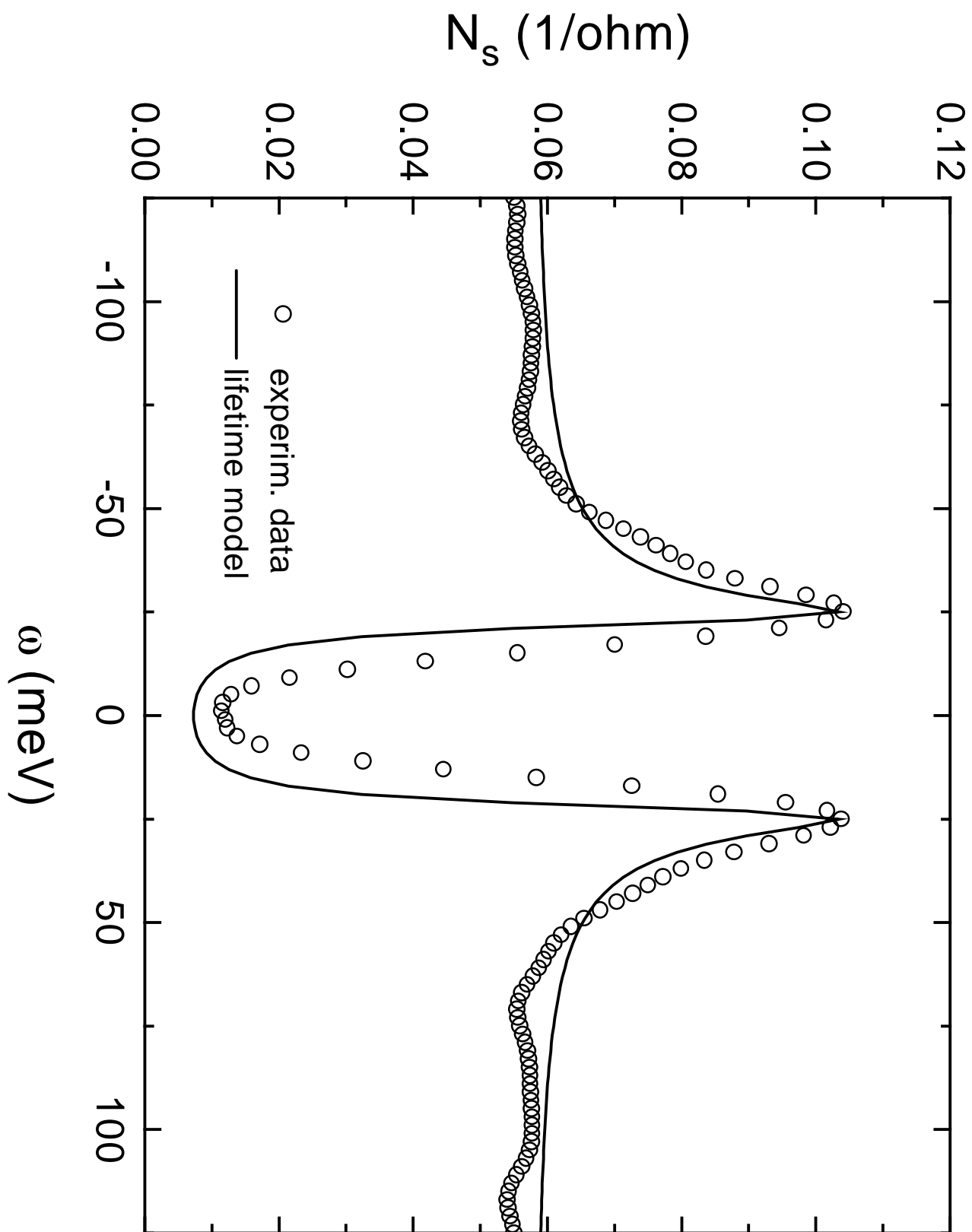
FIG. 4. (a) Comparison of the calculated DOS for $N_n(\omega) = \text{cost}$ (dash-dot line) with the experimental one determined from the data of Fig. 1 (open circles) and with the density of states calculated according to the NDOS exponential model of Eq. 3.1 (solid line). The BCS density of states (dash line) and the NDOS (dot line) are also shown for completeness; (b) The same as in (a) but for the linear model of the NDOS.

FIG. 5. (a) The same as in Figs. 4 (a) and 4 (b) but for the parabolic model of the NDOS; (b) The same as in (a) but for the lorentzian model of the NDOS.

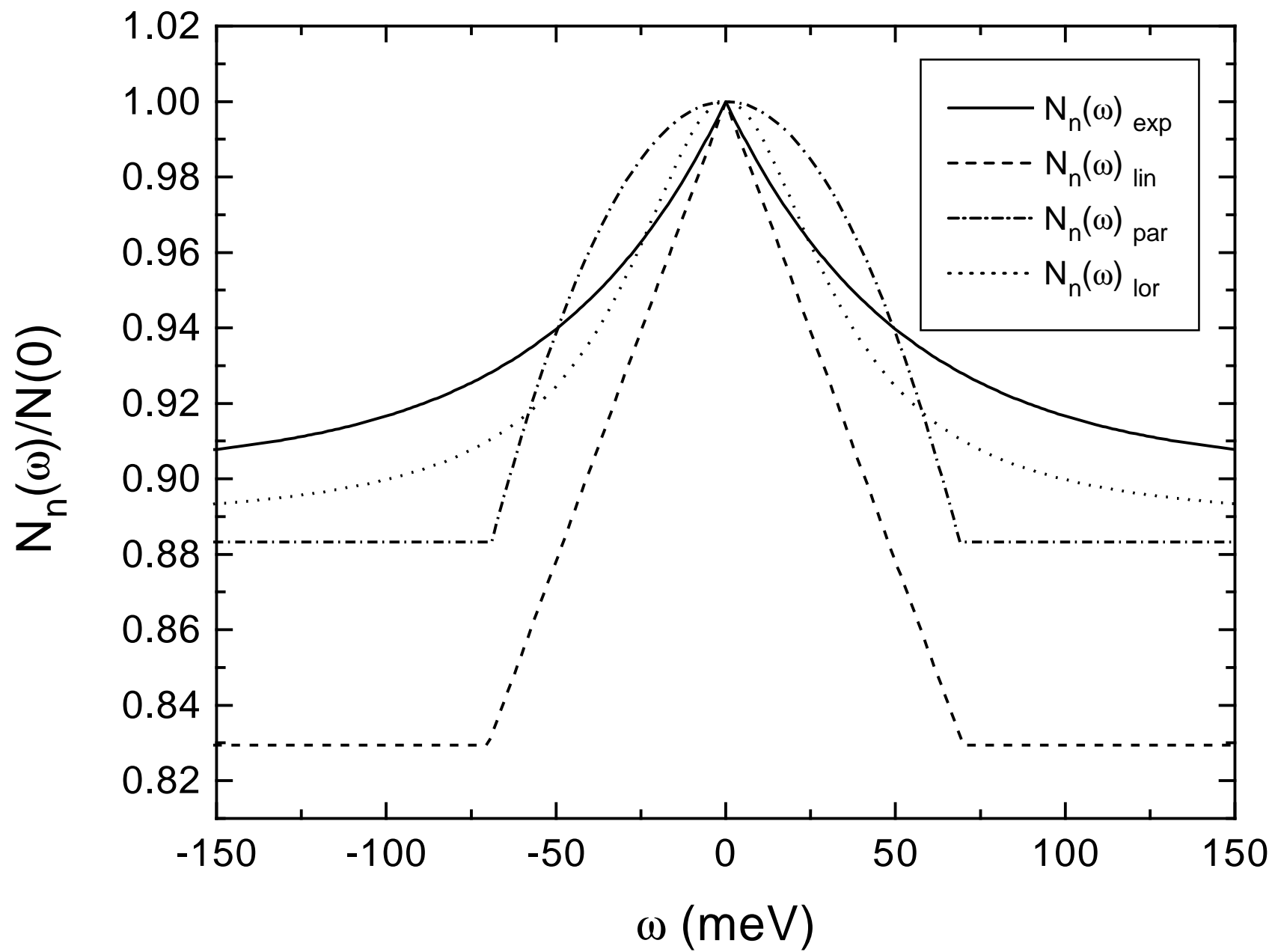
FIG. 6. Experimental DOS of BSCCO (open circles) compared to the theoretical electron density of states for the exponential NDOS model of Eq. 3.1 (solid line).

FIG. 7. Comparison of the effective electron-phonon spectral function (dash line) to the original $\alpha^2(\omega)F(\omega)$ determined from experimental data (solid line) and the neutron generalized phonon density of states (open circles).

FIG. 8. Comparison of the original $\alpha^2(\omega)$ determined from experimental data in the framework of exponential NDOS model (solid line) and the effective electron-phonon coupling function $\alpha^2(\omega)_{eff}$ (dash line).

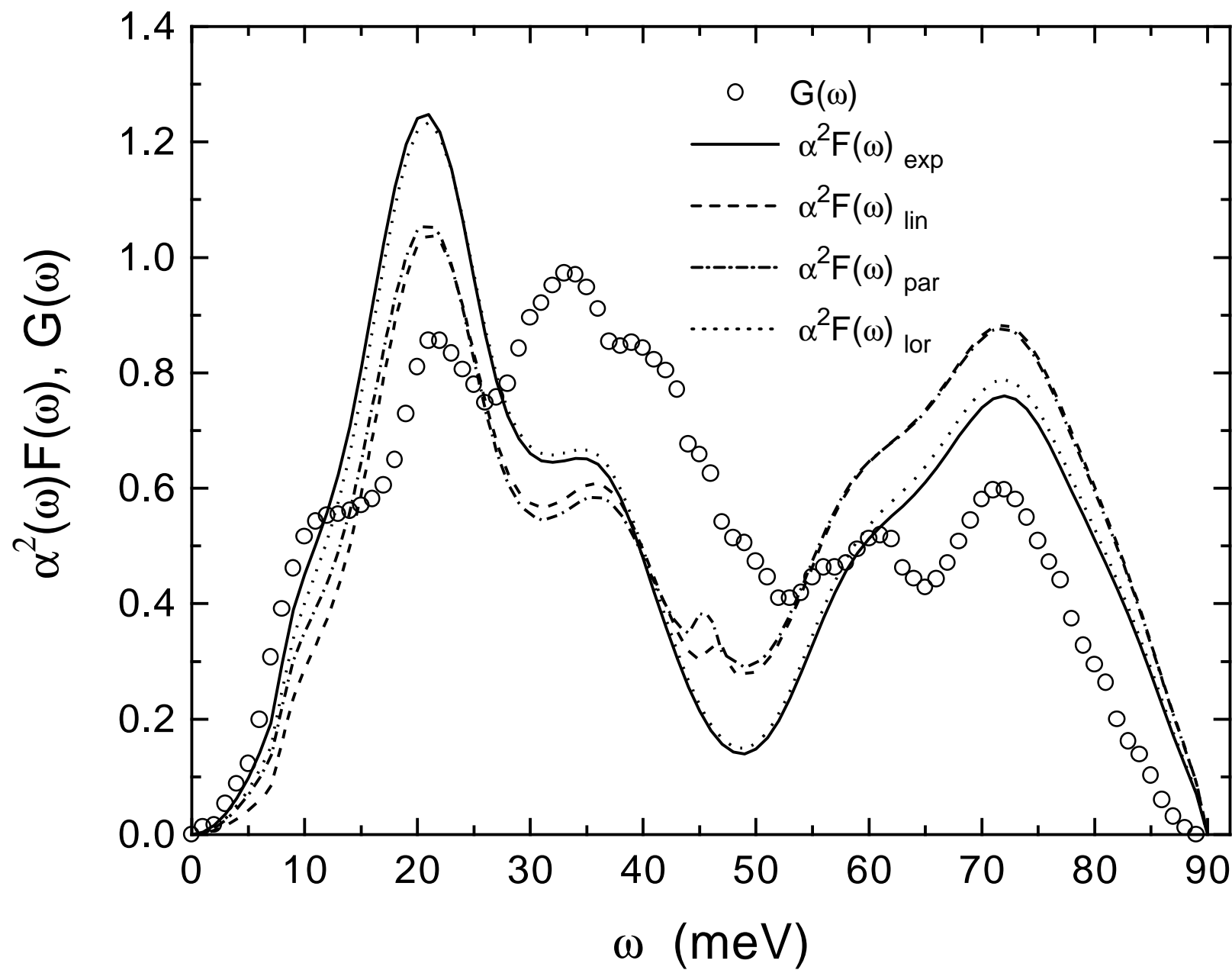


R. S. Gonnelli et al., "Determination of the tunneling electron-phonon ..."
 Fig. 1

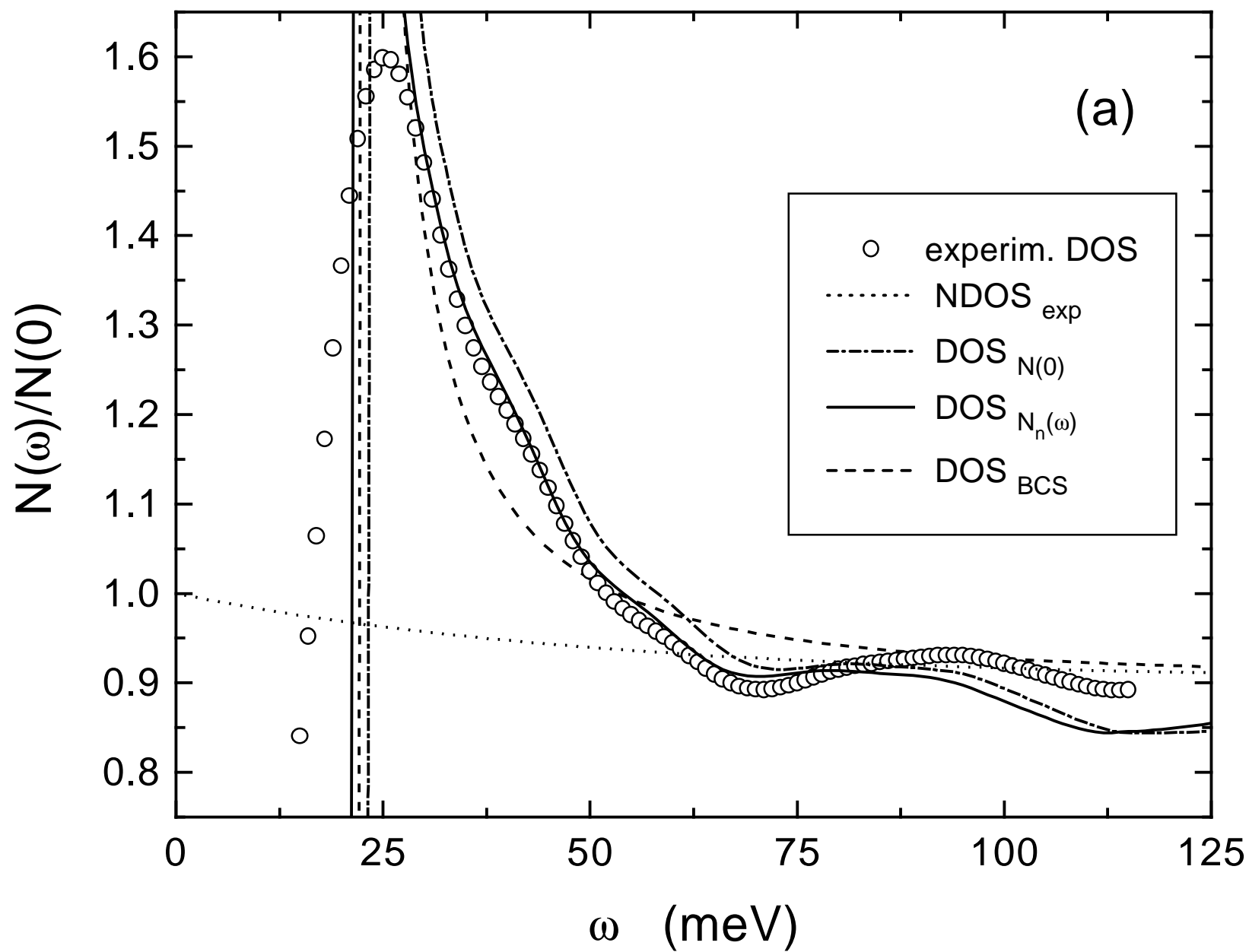


R. S. Gonnelli et al., "Determination of the tunneling electron-phonon ..."

Fig. 2

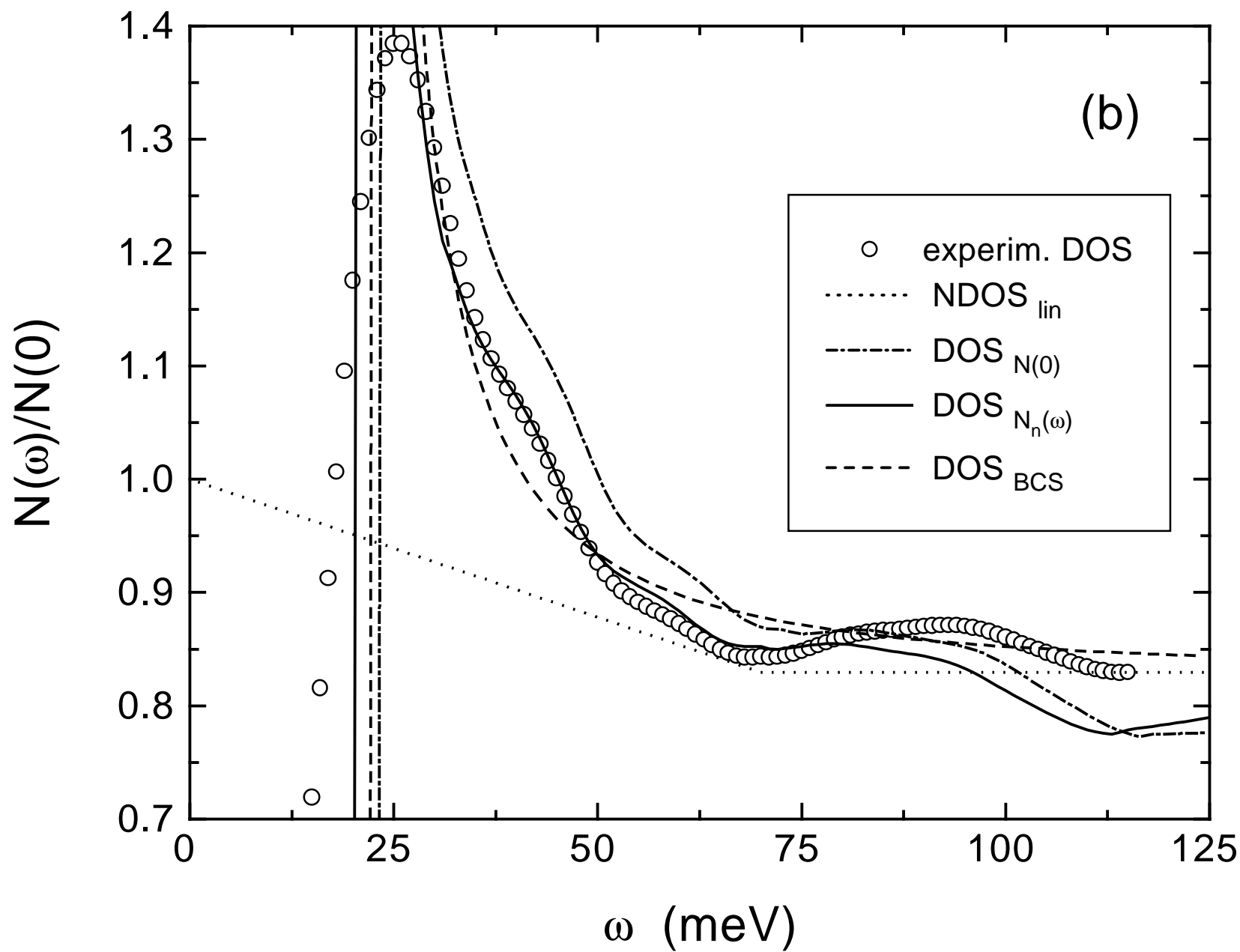


R. S. Gonnelli et al., "Determination of the tunneling electron-phonon ..."
Fig. 3

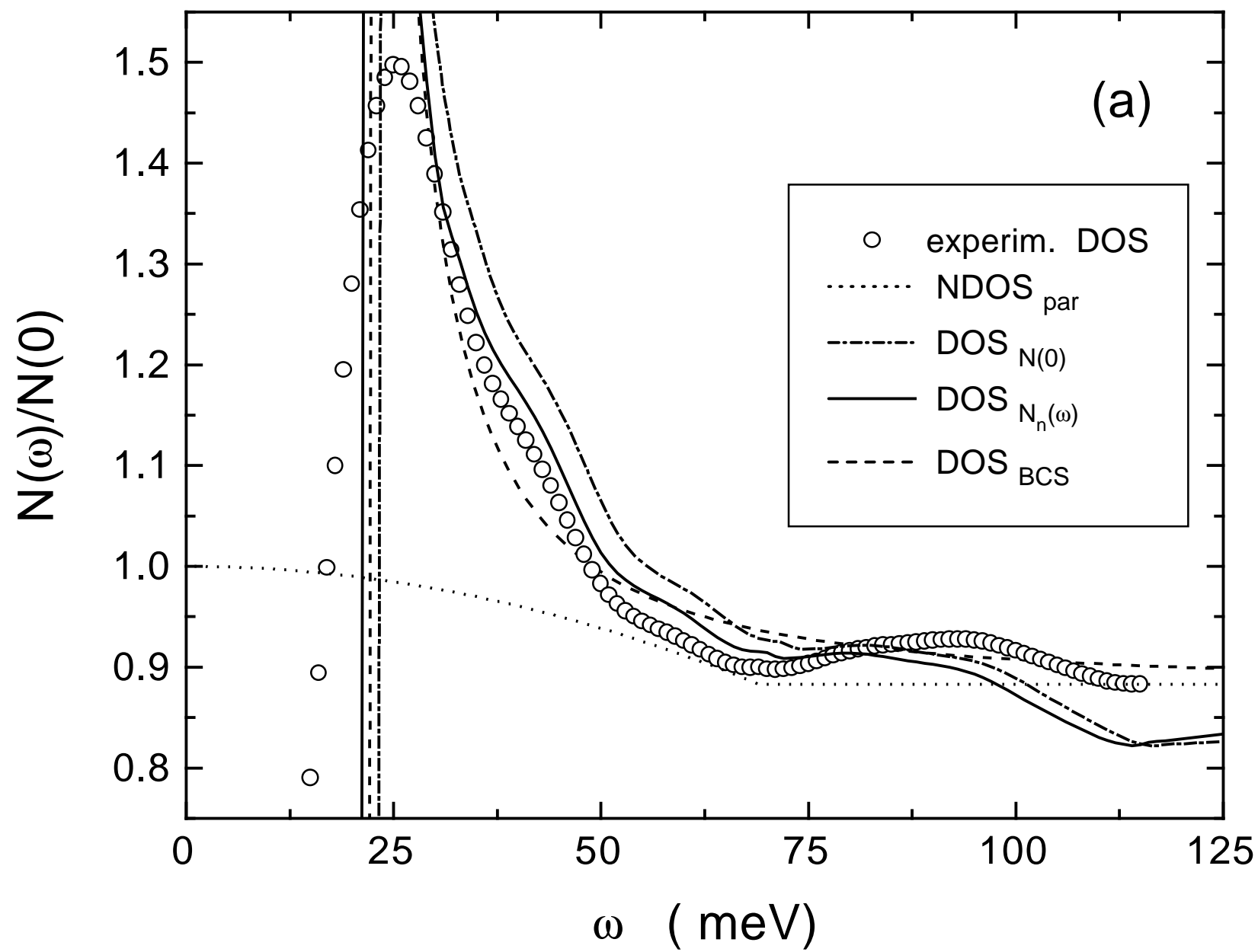


R. S. Gonnelli et al., "Determination of the tunneling electron-phonon ..."

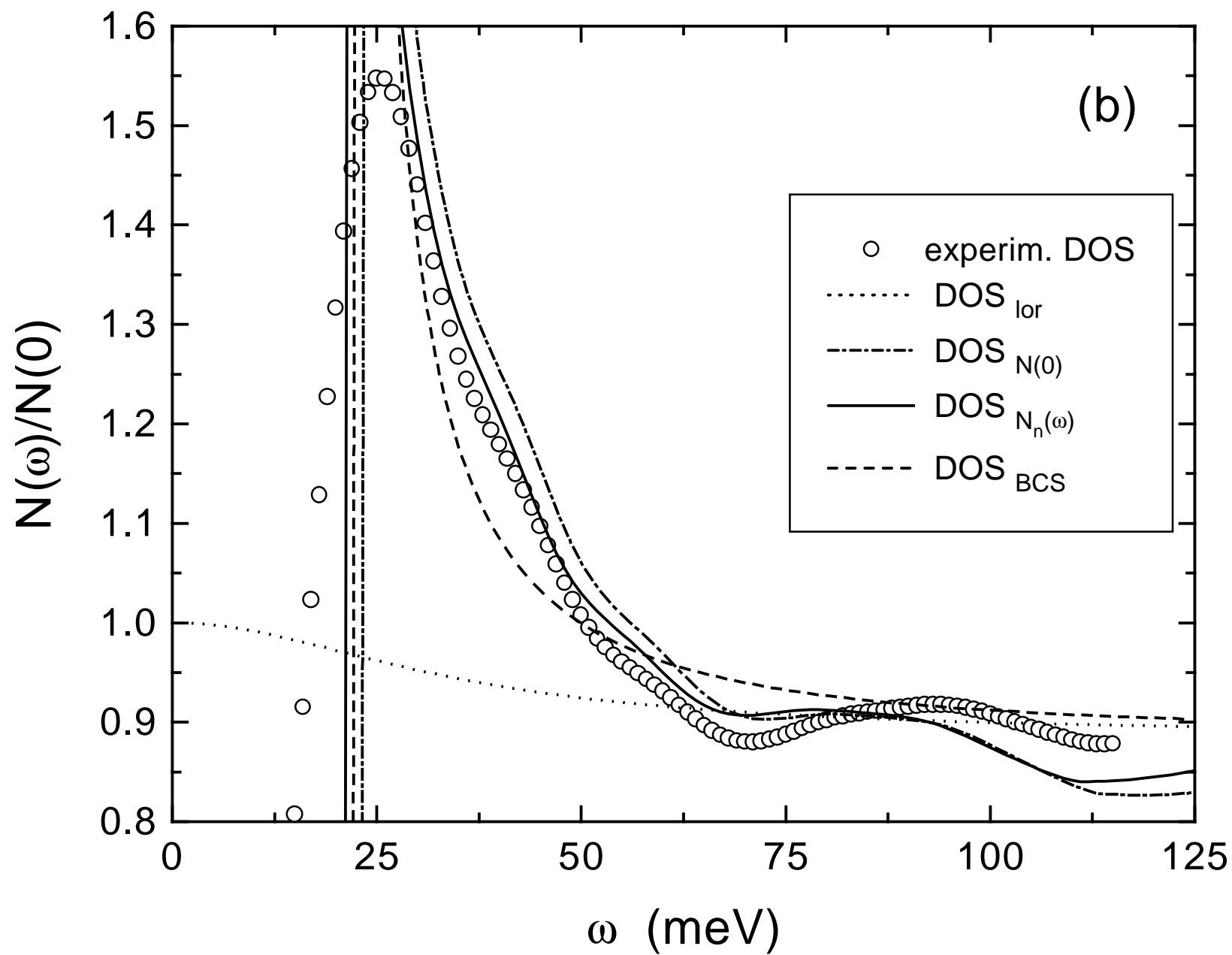
Fig. 4 (a)



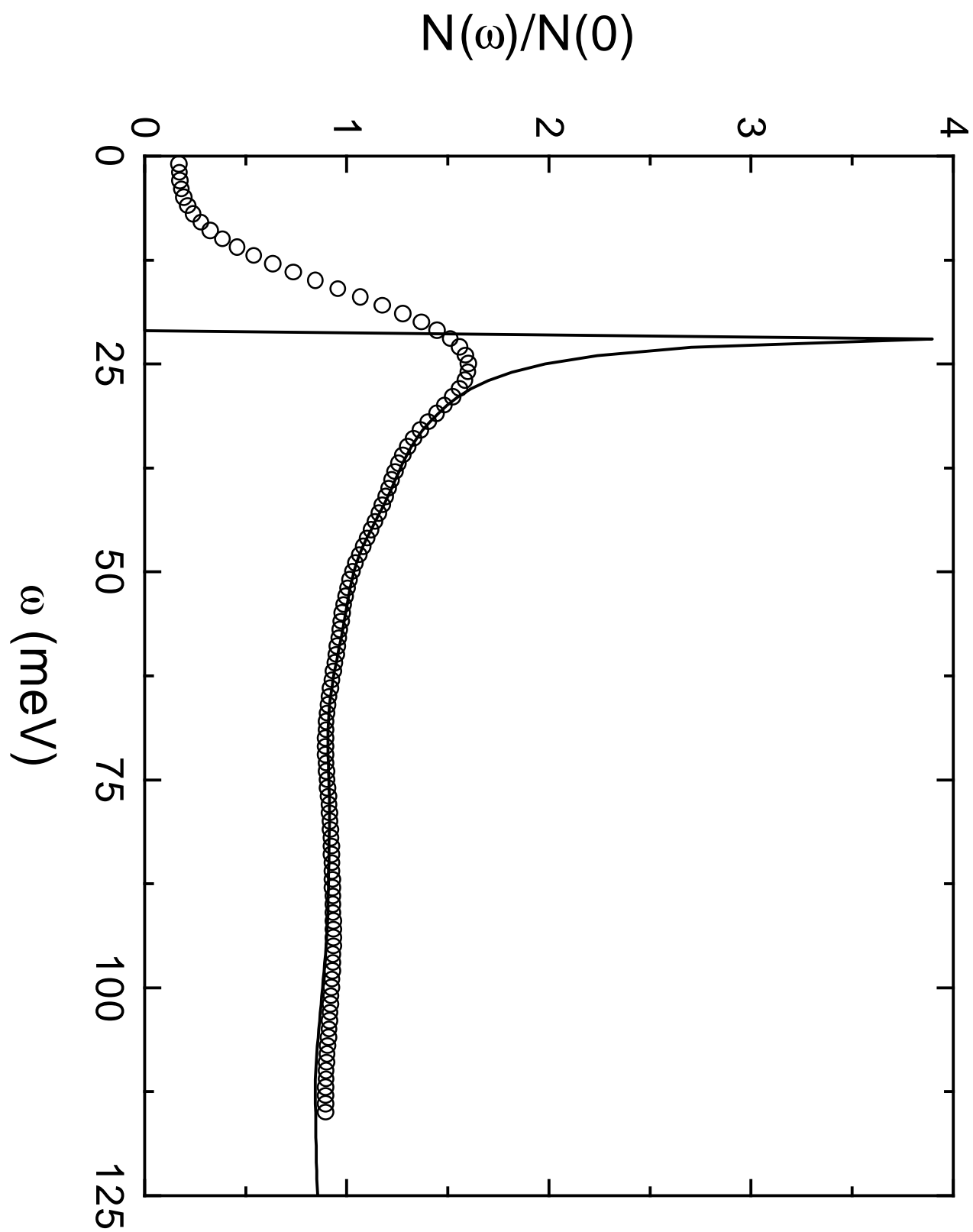
R. S. Gonnelli et al., "Determination of the tunneling electron-phonon ..."
 Fig. 4 (b)



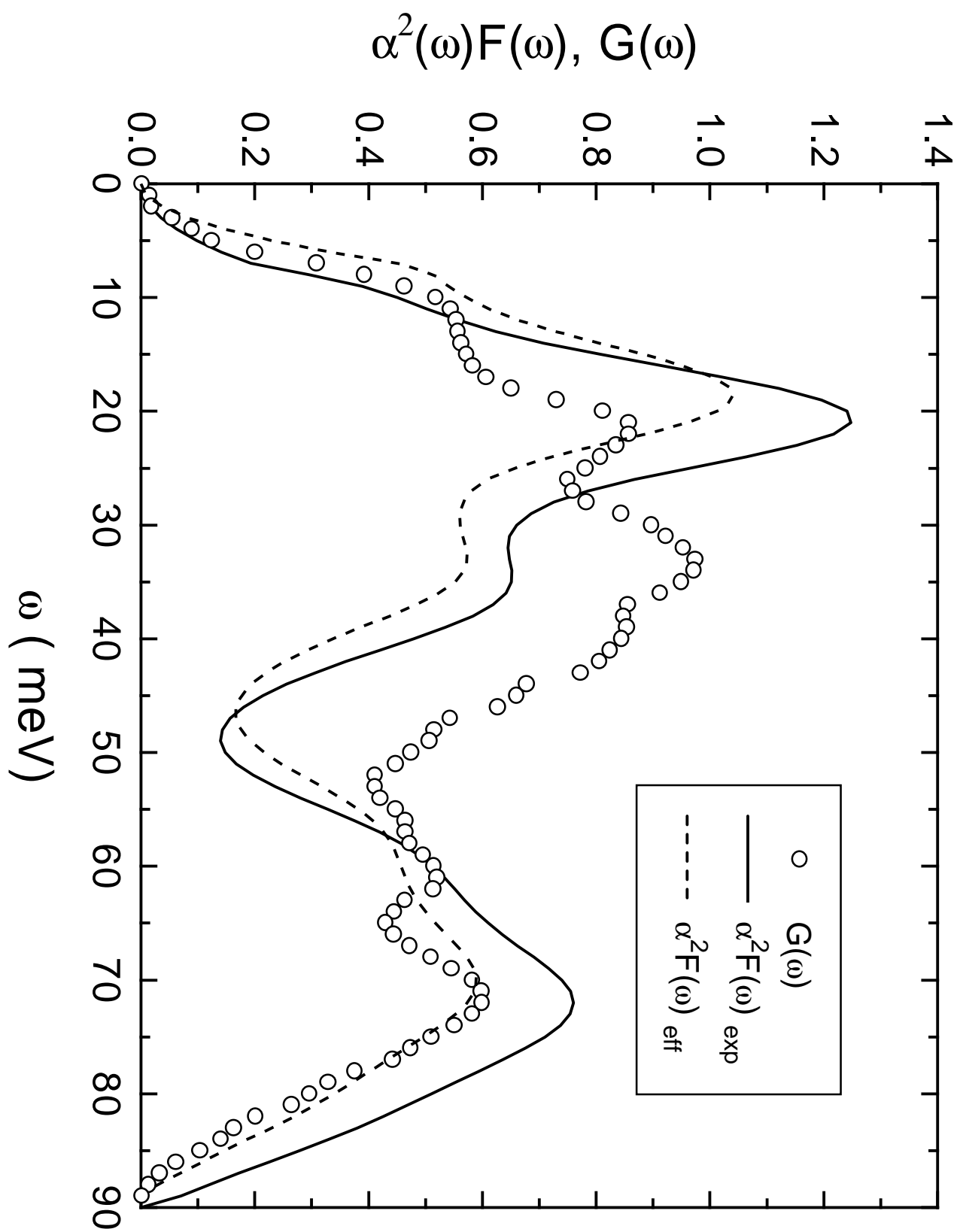
R. S. Gonnelli et al., "Determination of the tunneling electron-phonon ..."
Fig. 5 (a)



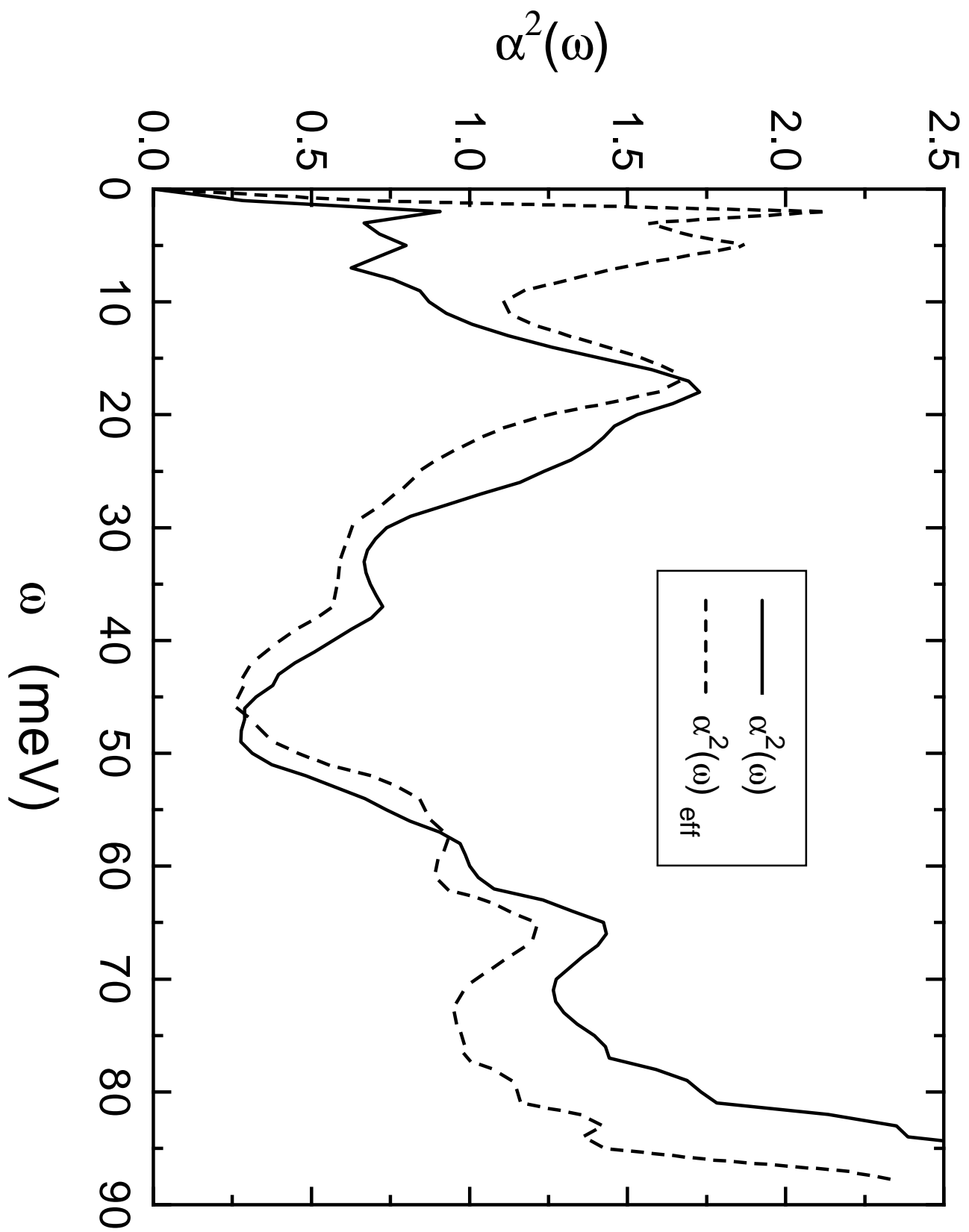
R. S. Gonnelli et al., "Determination of the tunneling electron-phonon ..."
 Fig. 5 (b)



R. S. Gonnelli et al., "Determination of the tunneling electron-phonon ..."
Fig. 6



R. S. Gonnelli et al., "Determination of the tunneling electron-phonon ..."
 Fig. 7



R. S. Gonnelli et al., "Determination of the tunneling electron-phonon ..."
 Fig. 8